An-Najah University Journal for Research – A
Natural Sciences

Flexural Performance of SCC Beams Reinforced with GFRP Rebars Containing EPS and Waste Plastic Fibers

Mohanad T. Abduljaleel[1,*] & Abdulkader Ismail Al-Hadithi[1,2]

(Type: Full Article). Received: 11st May. 2025. Accepted: 7th Oct. 2025, Published ××××, DOI: https://doi.org/10.xxxx

Accepted Manuscript, In Press

Abstract: This study aims to develop a modified self-compacting concrete incorporating expanded polystyrene (EPS) beads and recycled polyethylene terephthalate (PET) fibers to reduce density, improve ductility, and minimize environmental impact. Experimental work consists of five concrete beams of 150×200×1500 mm that have been designed and tested for studying the flexural behavior of steel and GFRP rebars of concrete beams under a three-point load setup. Adding a high content of cement and silica fume (SF) enhanced the flowability, also preventing the floating of EPS during mixing. This study focused on the impact of EPS and PET fiber. The results showed that partial replacement of the coarse aggregate with 0.17% EPS reduced the density and load capacity by 13.5% and 35.2%, respectively. In contrast, their ductility has been improved by 27.2%. The deflection has been reduced by 6% compared to the specimen without fiber, and the load capacity has improved by 15.6%. The steel reinforcement beam demonstrated different behavior with observed yielding, unlike the GFRP beam, which showed a higher load capacity, 42.4% more than the steel beam. Increasing the reinforcement ratio of GFRP raised the ultimate load capacity by 13.5% and decreased the deflection, strain, and ductility by 15%, 43%, and 13%, respectively. All GFRP beams showed a compression failure mode; in contrast, the steel beam showed a tension failure before the concrete crash. Comparing the test results with theoretical values of current commonly used specifications, it was found that the code predicts a more conservative moment capacity.

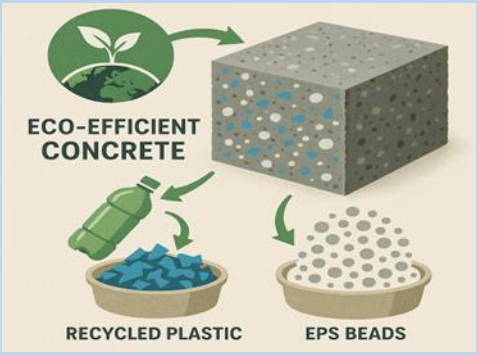

Keywords: Flexural behavior, Recycled PET fibers, Self-compacting concrete, GFRP, EPS.

Introduction

Particularly for concrete components with densely crowded reinforcements, self-compacting concrete (SCC) offers superior compaction, ease of pumping, and placement due to its extremely high fluidity [1]. SCC, one of the most recent developments in concrete technology, was initially discovered by Japanese scientists in the latter part of the 1980s. It is regarded as a concrete that can easily flow under its weight to fill the formwork and self-consolidate without experiencing any vibrations from machinery. This type of concrete must achieve magnificent deformability with great stability to ensure high filling capacity of the formwork with different shapes, deep and narrow sections, and congested structural members [2]. A significant distinction between SCC and traditional normal concrete is the increased volume of supplemental cementitious materials (SCM), such as fly ash (FA), blast-furnace slag (BFS), and silica fume (SF), that are incorporated into SCC. However, using wastes or by-products as substitute cementitious ingredients in concrete results in an eco-friendlier concrete by the establishment of a balance between the environment and development. Concrete's mechanical properties and durability are further enhanced by the addition of SCM to SCC combinations [3,4]. The numerous benefits of reinforced concrete make it a popular building material. However, many disadvantages, such as its low durability, restrict its application. Most often, the usage of steel reinforcement results in durability problems, which can be avoided by substituting the fiber-reinforced polymer, known as FRP, for steel. Fiber-reinforced polymers (FRPs) are typically composed of glass or carbon fibers embedded in a polymer matrix. The fibers provide tensile strength, while the matrix contributes to the bar's shape, shear capacity, and load transfer. Although FRP is non-corrosive compared to steel, its long-term durability may be affected by factors such as moisture exposure, elevated temperatures, and sustained loading [5–7]. The design philosophy of FRP states that the flexural strength of a member should exceed the factored moment, as expressed by the design criterion (ØMn ≥ Mu). The nominal moment capacity is typically determined using strain compatibility, internal force equilibrium, and the governing failure mode, either concrete crushing or FRP rupture [8].

$$M_n = \rho_f f_f \left(1 - 0.59\frac{\rho_f f_f}{f_c'}\right) bd^2 \quad (1)$$

$$\rho_f = \frac{A_f}{bd} \quad (2)$$

$$\rho_{fb} = 0.85\beta_1 \frac{f_c'}{f_{fu}} \frac{E_f \varepsilon_{cu}}{E_f \varepsilon_{cu} + f_{fu}} \quad (3)$$

$$f_f = \left(\sqrt{\frac{(E_f \varepsilon_{cu})^2}{4} + \frac{0.85\beta_1 f_c'}{\rho_f} E_f \varepsilon_{cu}} - 0.5 E_f \varepsilon_{cu}\right) \leq f_{fu} \quad (4)$$

1 Department of Civil Engineering, College of Engineering, University of Anbar, Anbar, Iraq
* Corresponding author email: moh22e1001@uoanbar.edu.iq
2 E-mail: abdulkader.alhadithi@uoanbar.edu.iq

The nominal flexural capacity of an FRP-reinforced concrete beam, M_n, is calculated using Eq. (1), which accounts for the actual FRP stress at ultimate conditions. The FRP reinforcement ratio, ρ_f, defined in Eq. (2) as the ratio of the FRP reinforcement area A_f to the product of beam width b and effective depth d, governs the failure mode. The balanced reinforcement ratio, ρ_{fb}, given in Eq. (3), represents the condition where concrete crushing in compression and FRP rupture in tension occur simultaneously. The actual FRP stress, f_f, at failure is obtained from Eq. (4) and is limited to the design tensile strength f_{fu}. This stress depends on the FRP modulus of elasticity E_f, the ultimate concrete compressive strain ε_{cu}, the equivalent rectangular stress block factorβ_1, and the concrete compressive strength f_c'. When ρ_f exceeds ρ_{fb}, the section is compression-controlled, with failure initiated by concrete crushing. Conversely, when ρ_f is less than ρ_{fb}, the section is tension-controlled, and FRP rupture governs the capacity. The main challenge in FRP design is its brittle failure. Incorporating randomly distributed microfibers into the concrete mix helps improve ductility and deformability in FRP-reinforced members [9,10]. Abed and Alhafiz (2019) demonstrated that incorporating basalt microfibers into BFRP-reinforced beams enhanced their flexural performance, with moment capacity gains of up to 19% compared to plain concrete, while ultimate compressive strain increased from 0.0031 to 0.0041. This improvement delayed concrete crushing, enabled fuller utilization of FRP tensile strength, and significantly refined crack control, maintaining crack widths below the serviceability limit of 0.7 mm [11]. Complementarily, Abed, El-Chabib, and AlHamaydeh (2012) provided one of the earliest systematic studies on the shear behavior of GFRP-reinforced deep beams without web reinforcement. Their results showed that although GFRP beams exhibited larger deflections (7–17 mm) than steel beams (4–12 mm) due to reduced axial rigidity, their ultimate shear capacities were comparable, and in high-strength concrete even 38% higher than steel counterparts. Moreover, shear capacity increased by 60% when the beam depth was enlarged by 33%, confirming the dominance of arch action in FRP-reinforced deep beams [12].

FRP rebars' inadequate ductility is their primary disadvantage, which in some circumstances would not be acceptable. The ductility of concrete elements can be increased in several ways [13]. Perhaps the most effective way is to incorporate polyethylene terephthalate (PET) [14]. Researchers have conducted a number of experiments to examine the effects of utilizing PET in concrete [15–22].

A novel lightweight material, which is appropriate for the construction sector, is expanded polystyrene (EPS). The mechanical characteristics of EPS concrete were experimentally studied. The testing results indicated that the mechanical features of EPS concrete are related to the EPS particle size and the granule content [23]. EPS has a bulk density of around 10.57 kg/m³. The mechanical properties of EPS were determined according to BS 8110-2:1985, which showed that the number of EPS beads influences the fresh and hardened properties. By incorporating 5% EPS, the compressive strength was 17 MPa at 28 days [24]. Concrete's density was significantly reduced when EPS and waste plastic fibers were used together; the largest decrease percentage was equivalent to 38.46%. Concrete prisms' flexural toughness increased when WPFs were used, the largest increase was equal to 180% when compared to those formed from the reference mix [25].

The main aim of this study is to develop a self-compacting concrete with improved ductility while reducing the environmental impact of waste materials through their incorporation into the mix. This modification also helps reduce the brittleness of GFRP failure.

Methodology

This study includes both collecting waste materials from the field and experimental work. In replacing the steel reinforcement with GFRP bars, an equivalent reinforcement ratio approach was used, keeping the total cross-sectional area of reinforcement (ρ) identical in both configurations. This ensured that the beams had the same geometric reinforcement level, enabling a direct comparison of material behavior.

Materials

Ordinary Portland cement type I was used for the production of SCC, which conformed to ASTM C 150 [26]. MegaAdd MS(D) silica fume (SF) was used as a high-performance pozzolanic mineral admixture in this study. It contains approximately 85% SiO_2 and has a bulk density of 700 kg/m³. SF functions chemically as a highly reactive pozzolan and physically by improving particle packing in the mortar or concrete. It conforms to ASTM C1240 standards [27]. In the experimental work, SCC was produced using a high-range water-reducing admixture (superplasticizer). Sika ViscoCrete 180 GS was used as the superplasticizer to enhance workability and flowability without increasing water content [28]. Natural normal-weight fine aggregate with a fineness modulus of 3.7 was used as fine aggregate, and crushed coarse aggregate with a maximum size of 10 mm was used to produce SCC, which followed ASTM C136 [29] and was consistent with ASTM C33 [30]. The commercially available spherical expanded polystyrene (EPS), as shown in Figure 1, was used as a lightweight aggregate in place of a partial replacement of the normal coarse aggregate. The grain diameter of EPS beads was mostly 5-10 mm, and the bulk density was 10 kg/m³. Waste plastic fiber, polyethylene terephthalate (PET), was used to improve load capacity and ductility. The properties of reinforcement bars and waste plastic fiber (PET) are demonstrated in Tables 1 and 2, respectively. Table 3 presents the mix proportion details, which include three mixes that have been matched to the EFNARC requirements [31]. The final three mix designs were selected after multiple trials to meet the required self-compacting concrete specifications, as shown in Figure 2.

Figure (1): Raw materials used in the concrete mix.

Figure (2): Fresh material test, (a) passing ability, (b) flowability.

Table (1): GFRP and steel rebars properties.

Diameter	Type	Yield Strength (MPa)	Ultimate Tensile Strength (MPa)	Elasticity Modulus (GPa)
6	Steel	570	670	200
10	Steel	625	703	200
10	GFRP	-	1100	45

Table (2): Plastic fiber (PET) properties.

Length (mm)	Width (mm)	Thickness (mm)	Aspect ratio	Tensile strength MPa	Elastic Modulus MPa
33	3	0.3	30	140	1000

Specimen details

For studying the flexural behavior of fibrous SCC containing EPS beads, three concrete beams with dimensions of 150×200×1500 mm have been designed according to ACI-4401R15 and ACI-318-19 [32,33]. The designed beam specimens were singly reinforced beams, with two 10 mm diameter GFRP bars at the tension zone and one 6 mm diameter as a hanger wire at the compression zone. The reference specimen is designed with two 10 mm diameter steel bars at the tension zone. The beam was provided with a concrete cover of 20 mm. The specimen was designed to resist shear failure when the longitudinal tensile reinforcement cracked to result in a flexural failure mode in the center of the beam. To avoid shear failure, a stirrup with a diameter of 6 mm was positioned at 65. The cross-sectional view of the concrete specimen is presented in Figure 3.

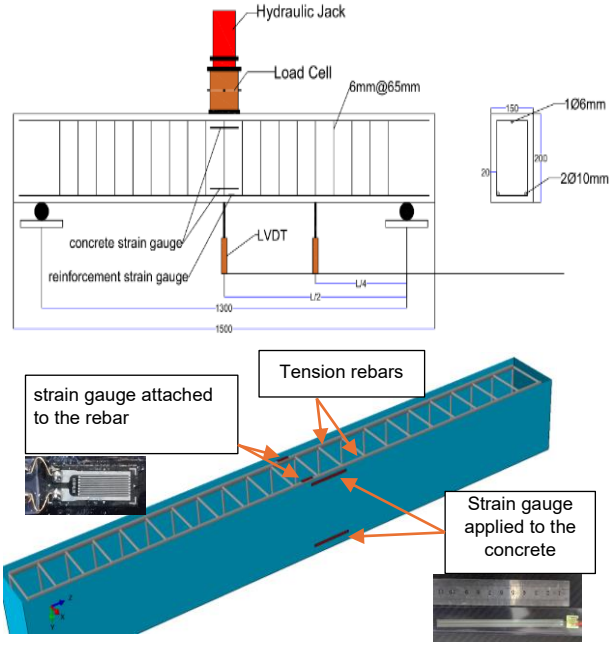

Figure (3): Details of reinforcement bars and equipment.

Table (3): Mix proportion details.

Material name*	Cement Kg/m³	Fine agg. Kg/m³	Course agg. Kg/m³	Water Kg/m³	SF Kg/m³	Fiber (PET) Kg/m³	SP Kg/m³	EPS Kg/m³	Limestone Powder Kg/m³
SCE	490	1100	400	189	100	-	12	2	-
SCEF	490	1100	400	189	100	5	13.7	2	-
SCR	250	980	700	210	-	-	9	-	230

Table (4): Properties of fresh and hardened chosen materials

No.	Material* name	Compressive Strength (MPa)	Tensile strength (MPa)	Modulus of rupture (MPa)	Density Kg/m³	Slump (mm)	T_{500} (S)	J-Ring (mm)	V-funnel (S)
1	SCE	21.5	2.7	2.875	1961	775	3	8	11
2	SCEF	22	3.3	2.908	1952	705	3	10	11
3	SCR	22.4	2.3	2.934	2301	750	2.1	9	9

*Material name (SCE); SC denotes self-compacting concrete, E indicates EPS, F indicates fiber, and R means reference without waste materials.

Beams casting

Wood plates were used to prepare the framework in accordance with the designed beam. A strain gauge with a resistance of 120 Ω was installed at the mid-span of the tension bar using a suitable adhesive. Prior to installation, the surface of the bar was prepared by polishing with fine sandpaper to remove impurities and ensure adequate bonding between the strain gauge and the substrate. According to the mix proportions as shown in Table 3, the concrete was correctly batched and mixed. The beam's framework was filled with concrete that had been mixed on a pan mixer. Sand and coarse aggregate were first dry-mixed with the cementitious materials. The superplasticizer was then diluted in water and added to the mix. Finally, EPS beads and fibers were gradually incorporated. The molds were filled with concrete and properly leveled. After 24 hours, the specimens were demolded and wrapped in wet gunny bags for continued curing. The experimental work is illustrated in Figure 4.

Figure (4): Details of experimental work, (a) reinforcement bars (b) concrete pouring.

Experimental Result and Discussion

The study's main goal is to test specimens under flexural loading in order to investigate the load-carrying capacity, moment versus deflection, ductility, cracking, and load-strain.

Material properties

Three different materials were chosen from Table 3, and they received numbers 1, 2, and 3, based on the results of fresh properties. Table 4 explains the details of the fresh properties of the designed materials. Figure 5 demonstrates the compressive strength with time, the distribution of the fibers, and EPS beads after the test.

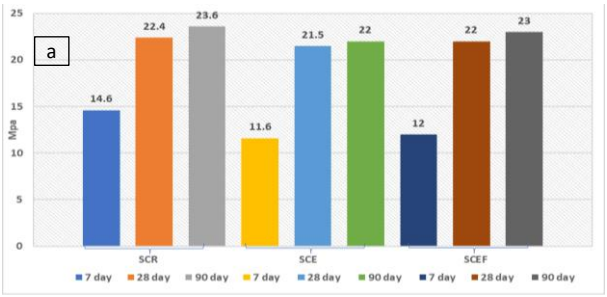

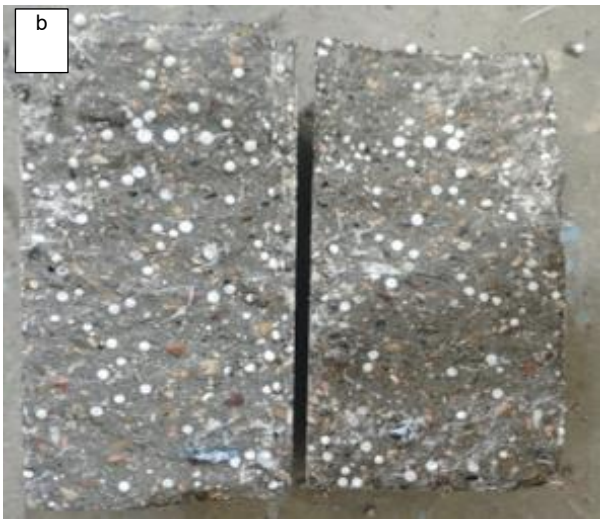

Figure (5): Shows (a) the compressive strength over the period, (b) the distribution of EPS after testing.

Load-carrying capacity

Table 5 presents the experimental results and theoretical load capacities of five concrete beams, including one beam reinforced with steel bars (SS) and four beams reinforced with GFRP bars. The performance of moment-displacement is presented in Figure 6, and it shows that the concrete beams with GFRP rebars carried a higher load up to failure compared with beams reinforced with steel bars. This result is attributed to the ability of GFRP bars to carry more tensile strength than steel bars. GFRP bars demonstrated an appropriate bonding throughout the experimental test, and no excessive cracking or spalling was observed during the visual monitoring. Increasing the reinforcement ratio considerably enhanced the load capacity compared with beams made of the same material. The GEFρ beam's load capacity grew by 13.5% when the reinforcement ratio was raised, compared with the GEF concrete beam. A similar observation was found by increasing the reinforcement ratio [34]. Despite having identical material properties, the SG specimen exhibited a 42.4% higher load capacity than the SS concrete beam. This enhancement is attributed to the mechanical behavior of GFRP bars and their superior ability to transfer stresses between the reinforcement and surrounding concrete. The behavior of all specimens was similar except for the specimen SS, which was reinforced with steel rebars. The moment-deflection curves of the two beams, SS and SG, reflect the difference between ductile steel reinforcement and brittle GFRP reinforcement. The load-deflection response of the steel-reinforced beam SS became flat after reaching 47.9 kN, suggesting that the steel bars yielded and the beam entered a plastic (ductile) state. The GFRP-reinforced beam (SG) showed a different behavior compared to steel-reinforced beams. It did not exhibit a yield point or a sudden drop in load during testing. Instead, it maintained a nearly linear and proportional response until failure. The beam also reached a higher peak load of 83.25 kN. In contrast, steel reinforcement is ductile and undergoes plastic deformation after yielding. The use of expanded polystyrene (EPS) beads in self-compacting concrete (SCC) reduced the load-carrying capacity of the beams. This is because EPS beads are lightweight and non-structural. Unlike natural aggregates, they do not contribute to strength and instead reduce the overall density of the concrete. This reduction in strength observed in the current study is in agreement with previous research findings [35, 36]. Concrete beam behavior was evidently improved and enhanced by waste plastic fiber (PET), specimens with identical material and reinforcing ratios (GE, GEF) showed a 15.6% improvement in load capacity when EPT was used. The increase in capacity for PET waste plastic fiber might be attributed to the fiber's capacity to transport and distribute stress across cracked zones by creating significant bridging between the concrete matrix. Researchers also found that using waste plastic as fiber increased members' load capacity [37–39]. Figure 6 shows that combining EPS beads and PET fibers reduced the load capacity by 23.3% when comparing SG and SGFE specimens. SG was made with a limestone-based reference mix (SCR), which performed better and was more economical. In contrast, SGFE used eco-efficient materials (EPS and PET), which led to lower strength despite their sustainability benefits.

Table (5): Experimental and theoretical results.

Beam's name	Reinforcement types	Material's name	Experimental load Capacity kN	Theoretical load capacity kN	Capacity ratio Exp./Theor.	Reinforcement Ratio
SS	Steel	SCR	47.9	46	1.04	0.62%
SG	GFRP	SCR	83.25	40	2.08	0.62%
SGE	GFRP	SCE	53.9	39	1.36	0.62%
GEF	GFRP	SCEF	63.9	39.5	1.6	0.62%
GEFρ	GFRP	SCEF	73.9	51.5	1.43	1.23%

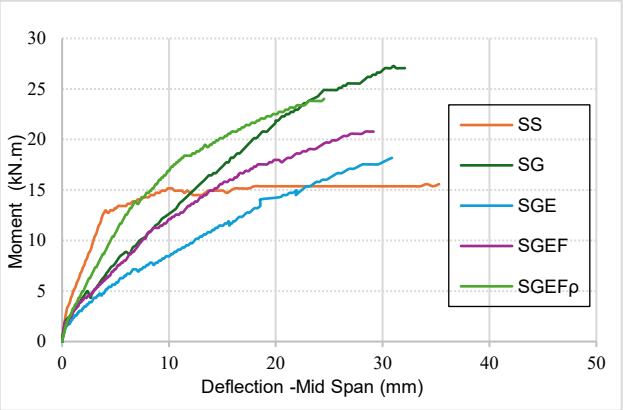

Figure (6): Moment-deflection curves.

Load-deflection properties

All concrete beams were tested under identical three-point bending conditions. Two LVDTs were positioned at mid-span and at L/4, as shown in Figure 7. The corresponding load–deflection curves and experimental results are provided in Figure 8 and Table 6. All specimens showed similar load–deflection behavior before the first crack, except for the SS reference beam reinforced with steel. The SS specimen exhibited a clear yield phase due to the ductile nature of steel, while the SG specimen, reinforced with FRP bars, showed no distinct yield and behaved in a linear-elastic manner until failure. As a result, the SG beam reached a higher ultimate load due to the high tensile strength of FRP but failed with limited ductility. The ductile response of the SS beam absorbs more energy (large post-yield deflections) and produces warning cracks before failure. The elastic modulus of FRP rebars, which is around one-fourth that of conventional steel reinforcement, is responsible for this phenomenon. In contrast to the SS specimen, which had a well-defined yielding with greater ductility, all specimens reinforced with GFRP bars displayed predictable linear behavior. The flexural capacity of the GFRP-reinforced specimens was 42.4% higher than that of the SS specimens. After the first crack, all specimens demonstrated similar load–deflection trends. To assess the effect of plastic fibers, specimens SGE and SGEF, having identical reinforcement ratios, were compared. The SGEF specimen exhibited higher load capacity, attributed to the inclusion of PET fibers. Additionally, increasing the GFRP reinforcement ratio in specimen SGEFρ resulted in noticeably stiffer behavior. Using waste plastic fiber (PET) improves stress distribution throughout the concrete matrix, resulting in a lower deflection value. Consequently, using waste plastic fiber contributes to the enhancement of the beam's stiffness and reduces beam deflection by 6%. The maximum midspan displacement of the specimens decreases by 15% with an increased reinforcement ratio. This result is in line with what other studies have found [40]. Consequently, the distribution of plastic fibers within the concrete beams may enhance the beams' overall performance and minimize beam deformations. Adding the EPS beads to the concrete has reduced the capacity of the concrete and changed the stiffness behavior. Using EPS as a partial replacement of coarse aggregate decreased the capacity by 35.25%.

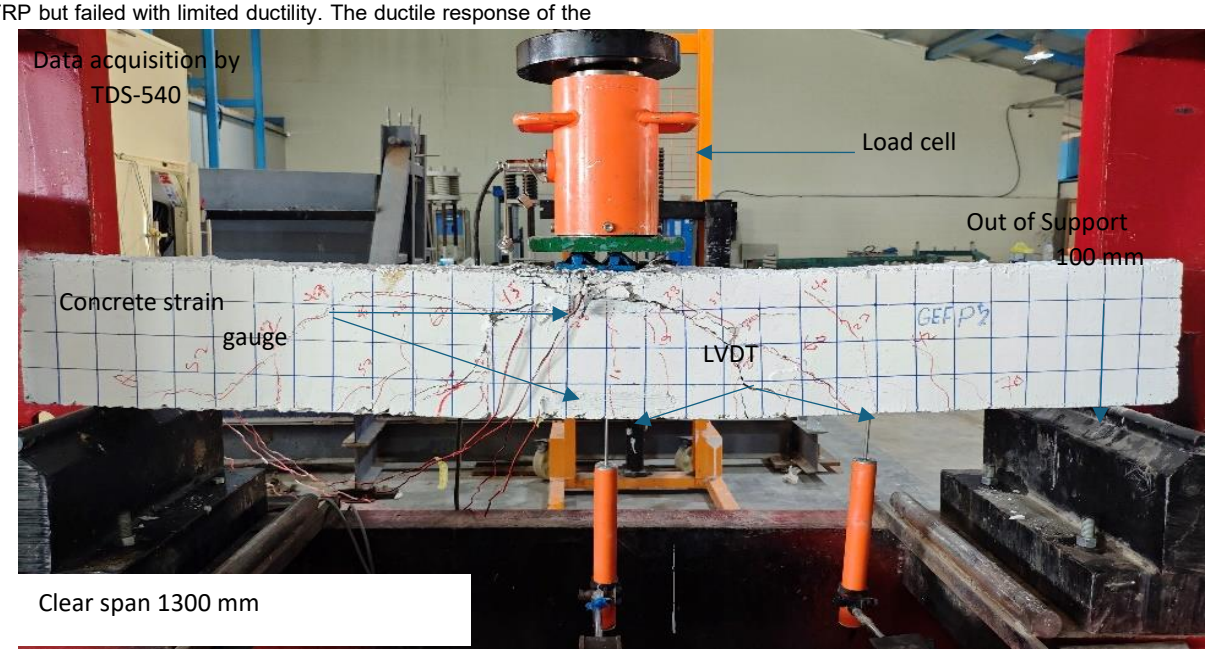

Figure (7): The test setup.

Table (6): The experimental data of five concrete Beams.

Beam's name	First crack load (kN) P_{cr}	Yielding load (kN) P_y	Ultimate load (kN) P_u	First crack deflection Δ_{cr}	Yielding deflection (mm) Δ_y	Ultimate deflection (mm) Δ_u	Ductility index	Failure mode
SS	10	40	47.9	0.5	4	34.5	2.5	T+C
SG	5.5	-	83.25	0.4	-	31	1.47	C
SGE	4.6	-	53.9	0.3	-	30.8	2.02	C
SGEF	6	-	63.9	0.25	-	29	2.3	C
SGEFρ	5	-	73.9	0.6	-	24.5	2	C

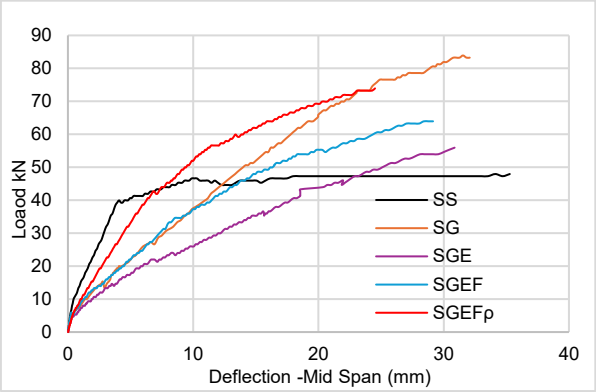

Figure (8): Load-deflection curves.

Load-strain responses

The load-strain behavior of all specimens is demonstrated in Figure 9. The response of load-strain for steel reinforcement and GFRP reinforcement was similar before the first crack, acting linearly elastic. After the first crack, the strain increased rapidly and showed a notable decrease in stiffness. For a similar reinforcement ratio of GFRP, specimens showed excessive strain before concrete cracking. Unlike steel reinforcement, GFRP performed linearly with load up to failure. Increased GFRP bar ratio for identical material decreased the strain by 43% due to the effect of stiffness improvement. Using PET fiber decreased the strain by 14.6% due to the enhancement of the concrete matrix. Similar to the load-deflection curves behavior, no yield point has been observed for the GFRP rebar specimens.

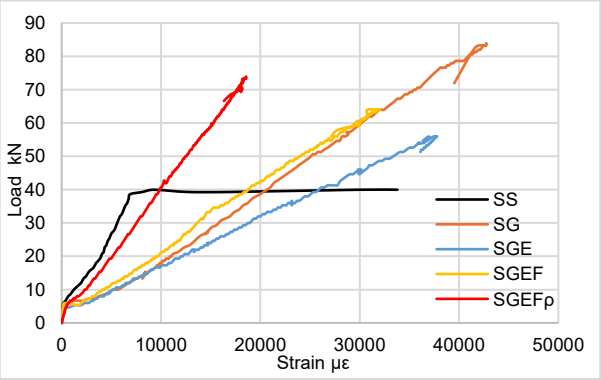

Figure (9): Load - strain of the rebars.

GFRP rebar showed 20% higher strain compared with steel rebar, due to the low modulus of elasticity value of GFRP bars. Due to its significantly lower modulus (40-60 GPa) compared to steel's (about 200 GPa), GFRP experiences a greater elastic deformation under the same load. Furthermore, strain increases are limited because steel yields and enters a plastic deformation phase. In contrast, GFRP bars retain linear-elastic behavior until failure, without yielding, allowing strain to increase proportionally with the applied load. Use of brittle, non-ductile materials requires careful design considerations; this basic difference in material behavior explains why GFRP reinforcement experiences greater strain. Figure 10 shows the concrete strain in both the compression and tension zones. A notable enhancement was observed when EPT fiber was added to the concrete matrix. The development of strain is attributed to the bridge between cracks by the advantage of fibers. Increasing GFRP bars reduced the concrete strain by 53.75%. Compared to steel reinforcement beams, the neutral axis for the GFRP specimens rose quickly for an identical reinforcement ratio, and the strain in concrete for both compression-tension zones increased rapidly, which was consistent with the previous study results [41] and [42]. The expanded polystyrene beads (EPS) showed more excessive strain than the reference beams; this increase probably reduced the brittleness of GRPP failure due to the high deformation before the concrete crash and introduced better behavior before the sudden collapse. Figure 11 illustrates the concrete strain distribution across the specimen depth. The influence of increasing the GFRP reinforcement ratio was evident in specimen SGEFρ, where the tensile strain was reduced by 40% compared to SGEF. A similar reduction was observed in the compression zone. This behavior may be attributed to the improved elastic modulus (E) resulting from the increased reinforcement.

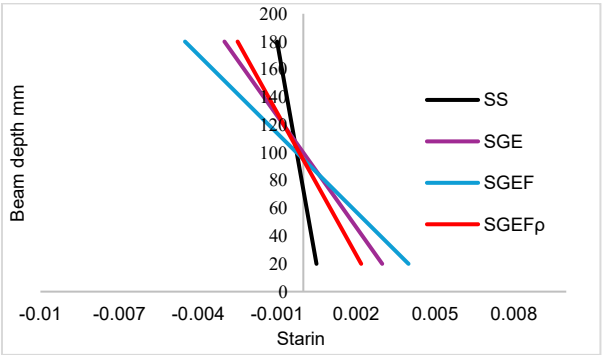

Figure (11): Concrete strain with height of the beam.

Failure mode and crack pattern

According to the experimental study, the failure mode for GFRP rebar specimens showed compression failure, while the steel reinforcement showed tension failure by steel reinforcement yielding (under reinforced) and concrete crushing. The three-point load technique partially affects the compression failure due to the concentrated load at one point, which was notable in the steel-reinforced beam, and is also attributed to the excessive deflection, which creates high stress at the top of the compression zone. Under identical loading tests, GFRP showed a high-capacity load due to the advantage of high tensile strength compared with steel bars. The first crack of GFRP beams was initiated at a load of 45% lower than that of a steel-reinforced beam because of the low modulus elasticity of GFRP

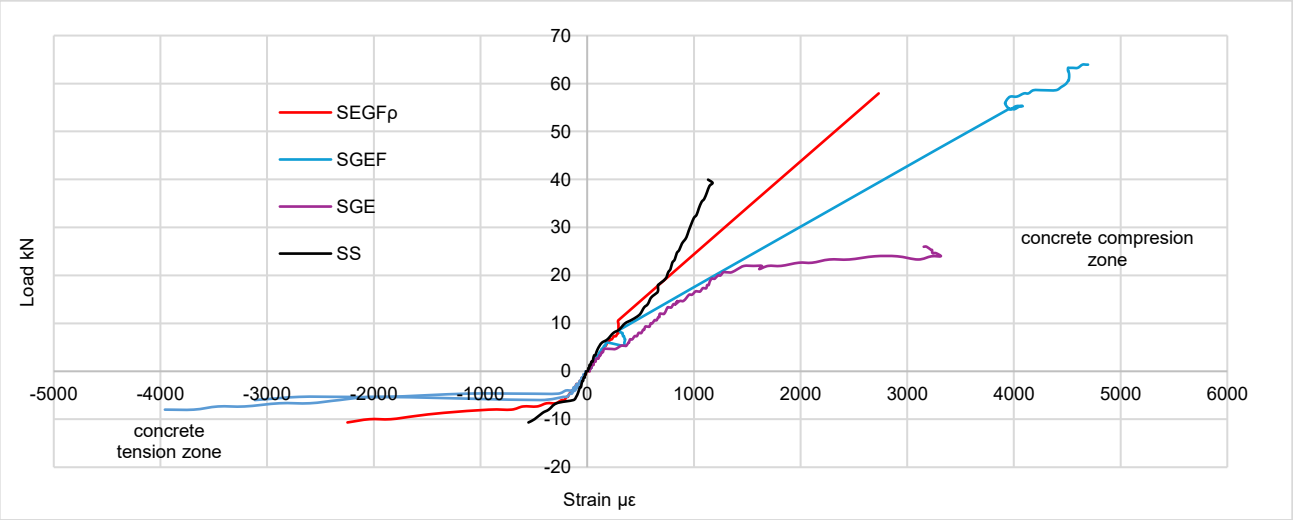

Figure (10): Load-strain of concrete beams.

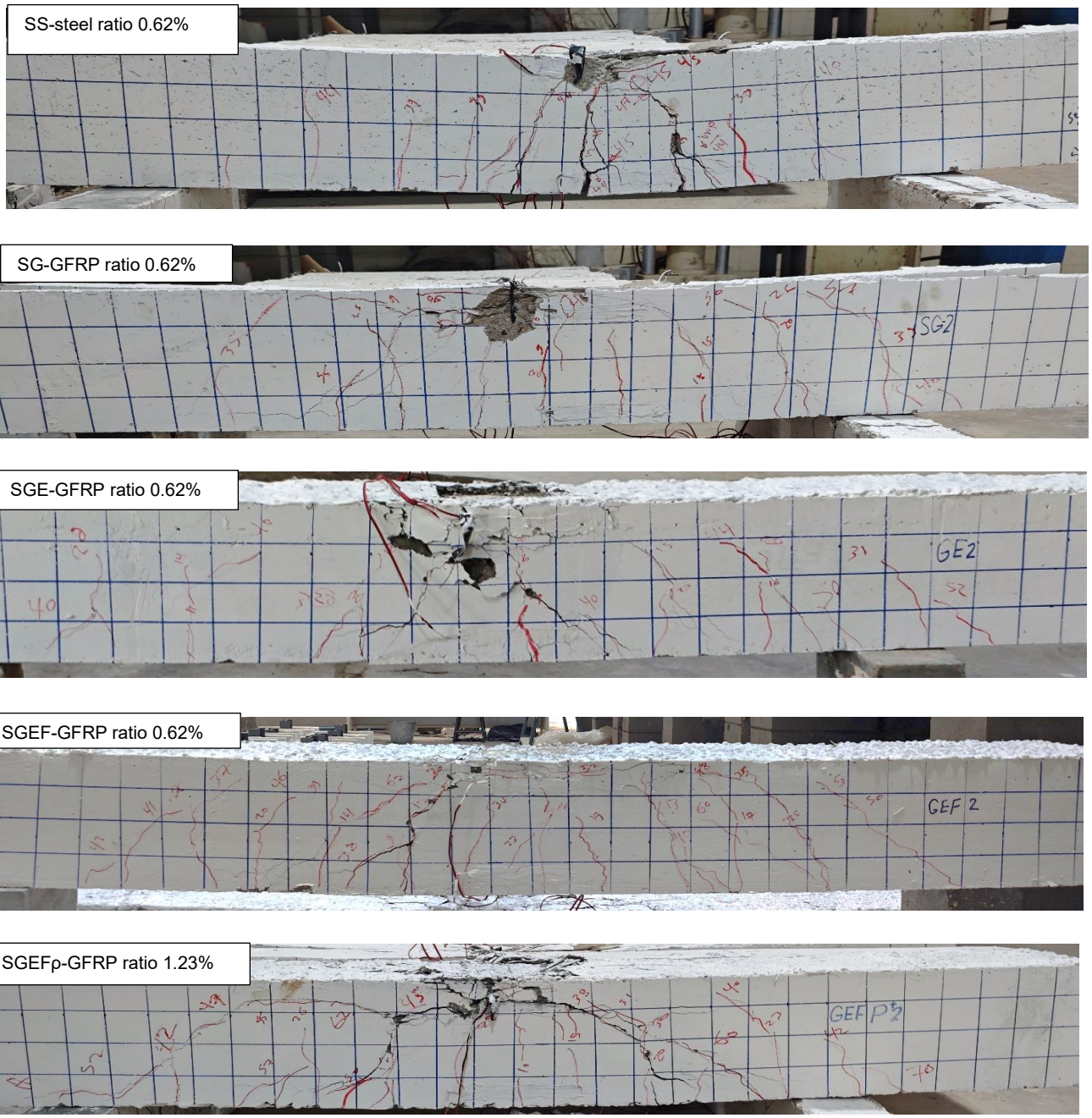

Figure (12): Cracking behavior and failure pattern.

Rebars. Figure 12 presents the experimental test of all specimens. Beams reinforced with GFRP rebars showed considerable compression failure, and the beam reinforced with steel rebars showed a notable tension failure. The deformability of GFRP specimens is higher than that of steel reinforcement due to the high stiffness of steel bars, which showed concentrated cracks in the bending section, compared to GFRP specimens, which showed different crack patterns by separation in the wider area. The first cracks of steel steel-reinforced beam appeared exactly under the concentrated load, unlike GFRP, which started behind the concentrated load, and this could be attributed to the high tensile strength of GFRP rebars. Increasing GFRP reinforcement ratio showed diagonal tension failure after compression failure due to the high confinement between the concentrated load and flexural reinforcement. When peak load was approached, the specimen reinforced with GFRP showed horizontal cracks in the compression zone, and the concrete was crushed after reaching the ultimate compressive strain, and this observation was noted by other studies [41]. Using PET fiber reduced the brittleness and changed the crack pattern; the SGEF specimen showed smooth cracks without spalling compared with the SGE specimen, and that was attributed to the (PET) fiber's performance, which was distributed uniformly throughout the concrete mixture's structure, increasing homogeneity and decreasing the number of voids inside the concrete and making it tougher and more adherent. The (PET) fibers attempt to stop the spread of microcracks in the surrounding region development and limit their spread once they start to form inside the matrix. Because of that, the crack propagation redirect becomes more intricate and requires more energy to continue [43]. Unlike the SGEF specimen, the SS beam showed a wide crack with a maximum value of 15 mm, and this was attributed to the modified SCC, which included fiber and expanded polystyrene beads (EPS). Despite the EPS beads minimizing the ultimate load capacity, but enhanced the mode of failure at the compression zone by absorbing energy and creating finer cracks. Positioning the EPS bead at the top fiber of the compression zone reduced the time of crack separation and delayed cracks before the ultimate load.

Ductility behavior

Ductility, which includes yielding and plastic behavior, represents the amount of plastic strain a member is resistant before failure. Deformability, on the other hand, describes the maximum amount of deformation an element can experience before failure, regardless of whether it has yielding or plastic behavior [44]. For adequate ductility, an elastic member should possess a higher reserve of strength than a ductile member (ACI Committee-4401R15, 2015). In the case of a steel-reinforced beam, the ratio of the yield deflection to the final deflection is known as the ductility index ($\mu\Delta = \Delta u/\Delta y$). Because the stress–strain properties of GFRP rebars lack the yield section of steel bars, the normal equation for calculating the ductility index of steel-reinforced concrete is not suitable for GFRP-reinforced concrete specimens. Therefore, Naaman and Jeong [45] suggested using the energy balance approach to determine the ductility of FRP-reinforced concrete specimens (see Eqs. (5,6)) [45]. Figure 13 provides a schematic representation of the ductility-index computation of FRP-RC specimens based on the energy calculation technique, using the load–deflection of the SGE beam as an example. The result of the ductility index is explained in Table 6. Using EPS beads improved elastic energy storage more quickly than total energy, while PET fiber increased the specimens' ductility, which was also found by other research [46]. The ductility of reinforced steel beams demonstrated the highest ductility index when compared to GFRP beams, and as a result, the ductility of GFRP beams decreases as the reinforcement ratio rises. These outcomes are consistent with the study's conclusions [41,47]. In summary, the steel bars exhibited significant deflection after the yielding point, resulting in a ductility index measuring 41.2% greater for SS beams than SG beams. Because the EPS beads minimized the rigidity, the SGE beam showed 27.2% higher ductility than the GS beam. PET fiber, which increased the overall energy, is responsible for the 12.17% improvement in SGEF beam ductility performance over the SGE beam because PET fibers bridge fractures, disperse stresses in the matrix, and limit the spread of cracks because of their high tensile strength, excellent flexibility, and elongation capacity. This behavior increases the ductility of the beams by increasing the deflection and number of fractures until the specimen fails, ultimately [48]. The GFRP beams' average ductility index value was 1.94, falling within the range of the indications that were noted [41,49]. Because the load–deflection curve of the GFRP specimens is basically bilinear, thus P1 = Pcr and P2 can be calculated from the slope inclination, which equals the point of intersection, as shown in Figure 13.

$$\mu = \frac{1}{2}\left(\frac{E_{total}}{E_{elastic}} + 1\right) \quad (5)$$

$$s = \frac{P_1 S_1 + (P_2 - P_1) S_2}{P_2} \quad (6)$$

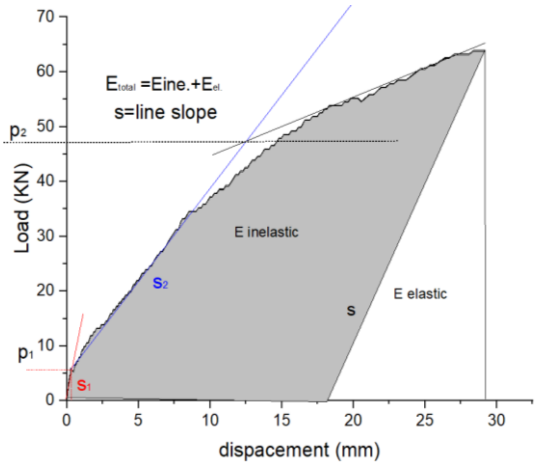

Figure (13): Example of the ductility index for beam SGE.

Conclusion

This study attempted to introduce the mechanical properties of SCC, which contained waste material (PET) and EPS, which already have a significant impact on the environment and require a significant period to dissolve. Five reinforced concrete beams with normal steel bars and GFRP rebars have been tested using the three-point load technique. The concrete density was (2227-1927) kg/m³, and the compressive strength was (21.5-22.5) MPa; the reinforcement ratio varied (0.62-1.23) %. The flexural load capacity, deflection, failure mode, and ductility of GFRP beams were analyzed, discussed, and compared with predictions from current codes. The main conclusions are summarized as follows:

1. The load capacity of GFRP-reinforced beams increased by 13.5% when the reinforcement ratio was doubled from 0.62% to 1.23%. In comparison, the steel-reinforced beam exhibited 42.2% lower capacity than the corresponding GFRP beam. The inclusion of EPS beads led to a 35.2% reduction in capacity, while adding PET waste fibers improved load capacity by 15.6%.
2. A notable 15% reduction in deflection was observed when the GFRP reinforcement ratio was increased. A similar trend was found with the addition of PET fibers, which led to a 6%

decrease in deflection. All specimens exhibited comparable load–deflection behavior, except for the steel-reinforced beam, which demonstrated significant yielding prior to failure.

3. The failure mode of the GFRP-reinforced beams was governed by concrete crushing, as the strain exceeded the ultimate compressive strain limit of the concrete. In contrast, the steel-reinforced beam failed due to the yield of the steel bars prior to concrete crushing. The crack pattern of GFRP-reinforced beams differed noticeably from that of steel-reinforced ones. The maximum crack width, measured at 15 mm, was observed in the steel-reinforced beam. The inclusion of EPS beads led to the formation of more distributed cracks, extending from the loading point toward the supports, due to the material's lightweight and low stiffness. The addition of PET fibers contributed to improved crack control by preventing spalling and enhancing the overall crack pattern. Furthermore, increasing the GFRP reinforcement ratio enhanced the confinement effect, resulting in the development of horizontal cracks in the compression zone.
4. The inclusion of EPS beads enhanced the ductility index, resulting in a 27.2% increase compared to the reference beam without EPS. In contrast, increasing the GFRP reinforcement ratio led to a reduction in ductility due to the brittle nature and lower modulus of elasticity of GFRP compared to steel. The steel-reinforced beam exhibited the highest ductility, attributed to the significantly higher modulus of elasticity (E) of steel. Additionally, the use of PET waste fibers further improved ductility, achieving a 12.17% increase relative to the beam without fibers.
5. The load-strain curves showed identical behavior compared to the load-deflection curves. For the same material, a higher GFRP bar ratio resulted in a 43% reduction in strain because of the improved stiffness. Because the PET fiber improved the concrete matrix, the strain was reduced by 14.6%. Since EPS exhibited more strain than the reference material, the significant deformation prior to concrete collision likely decreased the brittleness of the GRPP failure.
6. The design code, specifically ACI 440.1R-15, was found to provide conservative estimates of the moment capacity when compared to the experimental results. This suggests that the actual flexural performance of GFRP-reinforced SCC beams may exceed the predictions of current standard provisions.
7. The incorporation of 2 kg/m³ of EPS and 5 kg/m³ of recycled PET fibers in SCC offers a viable approach to reducing concrete density, minimizing environmental impact, and improving ductility without significantly compromising compressive strength.

Recommendations

1. Curing the EPS beads by coating the surface to increase the friction between the cement paste and EPS beads.
2. Using a high aspect ratio around 40 may enhance the load capacity.
3. It has been found that using the GFRP rebars with SCC (low-strength concrete 22 MPa, containing fibers and EPS) changed the failure mode from sudden collapse to giving an obvious warning. It is recommended to use the EPS as a layer in the tension zone and study the effect.

Disclosure Statement

The authors state that none of the work described in this study may have been influenced by any known conflicting financial interests or personal relationships.

- **Ethics approval and consent to participate:** This study did not involve human participants or animals.
- **Availability of data and materials:** The datasets generated and analyzed during the current study are available from the corresponding author on reasonable request.
- **Author's contribution:** The author conducted the experimental work, data analysis, and manuscript preparation. The author has read and approved the final manuscript.
- **Consent to participate Consent for publication:** Not applicable.
- **Conflicts of Interest:** The author declares that there are no conflicts of interest.
- **Funding:** This research received no specific grant from any funding agency in the public, commercial, or not-for-profit sectors.
- **Acknowledgements:** The authors are thankful to the excellent academic team of the University of Anbar for providing the necessary academic and technical assistance for this study.

Open Access

References

1] Saleh Ahari R, Erdem TK, Ramyar K. Permeability properties of self-consolidating concrete containing various supplementary cementitious materials. Constr Build Mater. 2015 Mar 15;79:326–36.

2] Erdem TK, Khayat KH, Yahia A. Correlating rheology of self-consolidating concrete to corresponding concrete-equivalent mortar. ACI Mater J. 2009;106(2):154.

3] Hassan AAA, Lachemi M, Hossain KMA. Effect of metakaolin and silica fume on the durability of self-consolidating concrete. Cem Concr Compos. 2012 Jul 1;34(6):801–7.

4] Şahmaran M, Yaman IÖ, Tokyay M. Transport and mechanical properties of self consolidating concrete with high volume fly ash. Cem Concr Compos. 2009 Feb 1;31(2):99–106.

5] Starkova O, Aniskevich K, Sevcenko J. Long-term moisture absorption and durability of FRP pultruded rebars. Mater Today Proc. 2021 Jan 1;34:36–40.

6] Clyne TW, Hull D. An Introduction to Composite Materials. An Introduction to Composite Materials. 2019 Jul 11;

7] Ceroni F, Cosenza E, Gaetano M, Pecce M. Durability issues of FRP rebars in reinforced concrete members. Cem Concr Compos. 2006 Nov 1;28(10):857–68.

8] ACI CODE-440.11-22. Building Code Requirements for Structural Concrete Reinforced with Glass Fiber-Reinforced Polymer (GFRP) Bars-Code and Commentary. 2022.

9] Bakis CE, Bank LC, Brown VI, Cosenza E, Davalos JF, Lesko JJ, et al. Fiber-reinforced polymer composites for construction—State-of-the-art review. Journal of composites for construction. 2002;6(2):73–87.

10] Wang H, Belarbi A. Ductility characteristics of fiber-reinforced-concrete beams reinforced with FRP rebars. Constr Build Mater. 2011;25(5):2391–401.

11] Abed F, Alhafiz AR. Effect of basalt fibers on the flexural behavior of concrete beams reinforced with BFRP bars. Compos Struct. 2019;215:23–34.

12] Abed F, El-Chabib H, AlHamaydeh M. Shear characteristics of GFRP-reinforced concrete deep beams without web reinforcement. Journal of Reinforced Plastics and Composites. 2012;31(16):1063–73.

13] Renić T, Kišiček T. Ductility of concrete beams reinforced with frp rebars. Buildings. 2021 Sep 1;11(9).

14] Jain A, Siddique S, Gupta T, Jain S, Sharma RK, Chaudhary S. Evaluation of concrete containing waste plastic shredded fibers: Ductility properties. Structural Concrete. 2021 Feb 1;22(1):566–75.

15] Shen L, Worrell E, Patel MK. Environmental impact assessment of man-made cellulose fibres. Resour Conserv Recycl. 2010 Dec 1;55(2):260–74.

16] Hopewell J, Dvorak R, Kosior E. Plastics recycling: Challenges and opportunities. Philosophical Transactions of the Royal Society B: Biological Sciences. 2009 Jul 27;364(1526):2115–26.

17] Pereira De Oliveira LA, Castro-Gomes JP. Physical and mechanical behaviour of recycled PET fibre reinforced mortar. Constr Build Mater. 2011 Apr 1;25(4):1712–7.

18] Ochi T, Okubo S, Fukui K. Development of recycled PET fiber and its application as concrete-reinforcing fiber. Cem Concr Compos. 2007 Jul 1;29(6):448–55.

19] Silva DA, Betioli AM, Gleize PJP, Roman HR, Gómez LA, Ribeiro JLD. Degradation of recycled PET fibers in Portland cement-based materials. Cem Concr Res. 2005 Sep 1;35(9):1741–6.

20] Foti D. Use of recycled waste pet bottles fibers for the reinforcement of concrete. Compos Struct. 2013 Feb 1;96:396–404.

21] Foti D. Preliminary analysis of concrete reinforced with waste bottles PET fibers. Constr Build Mater. 2011 Apr 1;25(4):1906–15.

22] Borg RP, Baldacchino O, Ferrara L. Early age performance and mechanical characteristics of recycled PET fibre reinforced concrete. Constr Build Mater. 2016 Apr 1;108:29–47.

23] Liu N, Chen B. Experimental study of the influence of EPS particle size on the mechanical properties of EPS lightweight concrete. Constr Build Mater. 2014 Oct 15;68:227–32.

24] ADEALA AJ, SOYEM OB. Structural Use of Expanded Polystyrene Concrete. Int J Innov Sci Res Technol. 2020 Jul 10;5(6):1131–8.

25] Al-Hadithi AI, Hilal NN, Al-Gburi M, Midher AH. Structural behavior of reinforced lightweight self-compacting concrete beams using expanded polystyrene as coarse aggregate and containing polyethylene terephthalate fibers. Structural Concrete. 2023 Oct 1;24(5):5808–26.

26] ASTM C150-07. Standard Specification for Portland Cement. American Society for Testing and Materials. 2007.

27] ASTM C 1240 – 05. Standard Specification for Silica Fume Used in Cementitious Mixtures 1. 2009.

28] EFNARC. Specification and Guidelines for Self-Compacting Concrete. 2002.

29] ASTM C 136 – 06. Test Method for Sieve Analysis of Fine and Coarse Aggregates. 2006 Feb 15;

30] ASTM C 33/C 33M. Specification for Concrete Aggregates. 2018 Mar 15;

31] EFNARC. The European Guidelines for Self-Compacting Concrete. 2005.

32] ACI 440.1R-15. Guide for the design and construction of structural concrete reinforced with fiber-reinforced polymer (FRP) bars. American Concrete Institute. 2015;

33] ACI 318M-19. Building Code Requirements for Structural Concrete. 318-19 Building Code Requirements for Structural Concrete and Commentary. American Concrete Institute; 2019.

34] Alkubaisi MG, Alhadithy AI, Mahmoud AS. Flexural behavior of beams reinforced by GFRP bars with CFRP sheets immersed in epoxy as shear. IRAQI JOURNAL OF CIVIL ENGINEERING. 2019;13–4.

35] Sayadi AA, Tapia J V., Neitzert TR, Clifton GC. Effects of expanded polystyrene (EPS) particles on fire resistance, thermal conductivity and compressive strength of foamed concrete. Constr Build Mater. 2016 Jun 1;112:716–24.

36] Duan P, Song L, Yan C, Ren D, Li Z. Novel thermal insulating and lightweight composites from metakaolin geopolymer and polystyrene particles. Ceram Int. 2017 Apr 15;43(6):5115–20.

37] Jouyandeh RT, Hemmati A, Mortezaei A. Using woven recycled plastic fibers in reinforced concrete beams. Constr Build Mater. 2023 Nov 10;404.

38] Khalid Ali O, Ismail Al-Hadithi A, Tareq Noaman A. Flexural performance of layered PET fiber reinforced concrete beams. Structures. 2022 Jan 1;35:55–67.

39] Al-Hadithi AI, Al-Waysi SY. The Effects of Adding Polymer and Waste Plastic Fibers on the Flexural Behavior of Reinforced Concrete Beams.

40] Saatci S, Vecchio FJ. Effects of shear mechanisms on impact behavior of reinforced concrete beams. ACI Struct J. 2009 Jan 1;106(1):78–86.

41] Li X, Zhang W, Zhang C, Liu J, Li L, Wang S. Flexural behavior of GFRP and steel bars reinforced lightweight ultra-high performance fiber-reinforced concrete beams with various reinforcement ratios. Structures. 2024 Dec 1;70.

42] Zhang Y, Zhu Y, Qiu J, Hou C, Huang J. Impact of reinforcing ratio and fiber volume on flexural hardening behavior of steel reinforced UHPC beams. Eng Struct. 2023 Jun 15;285:116067.

43] Al-Hadithi AI, Abdulrahman MB, Al-Rawi MI. Flexural behaviour of reinforced concrete beams containing waste plastic fibers. In: IOP Conference Series: Materials Science and Engineering. Institute of Physics Publishing; 2020.

44] Oudah F, El-Hacha R. A new ductility model of reinforced concrete beams strengthened using Fiber Reinforced Polymer reinforcement. Compos B Eng. 2012 Dec 1;43(8):3338–47.

45] Naaman A JS. Structural ductility of concrete beams prestressed with FRP tendons. Proc Second Int RILEM Symp (FRPRCS-2): Non-Met (FRP) Concr Struct, Ghent, Belg. 1995;86–379.

46] Ali H. Allawi AIAH, ASM. Effects of Waste Plastic PET Fibers on The Fresh and Hardened of Normal Concrete. IRAQI JOURNAL OF CIVIL ENGINEERING. 2021;

47] Peng F, Deng J, Fang Z, Tang Z. Ductility evaluation and flexural failure mode recognition of reinforced Ultra-High performance concrete flexural members. Structures. 2023 May 1;51:1881–92.

48] Medher AH, Al-Hadithi AI, Hilal N. The Possibility of Producing Self-Compacting Lightweight Concrete by Using Expanded Polystyrene Beads as Coarse Aggregate. Arab J Sci Eng. 2021 May 1;46(5):4253–70.

49] Yoon YS, Yang JM, Min KH, Shin HO. Flexural strength and deflection characteristics of high-strength concrete beams with hybrid FRP and steel bar reinforcement. Special Publication. 2011;275:1–22.